

HEMODYNAMIC FEATURES EXTRACTION FROM A NEW ARTERIAL PRESSURE WAVEFORM PROBE

V. G. Almeida, P. Santos, E. Figueiras, E. Borges, T. Pereira, J. Cardoso, C. Correia
Centro de Instrumentação (GEI-CI), University of Coimbra, Coimbra, Portugal

H. C. Pereira
Centro de Instrumentação (GEI-CI), University of Coimbra, Coimbra, Portugal
ISA- Intelligent Sensing Anywhere, Coimbra, Portugal

Keywords: Arterial pressure waveform, First derivative, Pulse contour analysis, Systolic peak, Dicrotic notch, Dicrotic peak and reflection point.

Abstract: In this work, we discuss an algorithm that reliably and accurately identifies the prominent points of the cardiac cycle: the systolic peak (SP), reflection point (RP), dicrotic notch, (DN) and dicrotic peak (DP). The prominent point's identifier algorithm (PPIA) action is based on the analysis a number of features of the arterial pressure waveform and its first derivative, and is part of the fundamental software analysis pack for a new piezoelectric probe designed to reproduce the arterial pressure waveform from the pulsatile activity taken non-invasively at the vicinity of a superficial artery. The output PPIA is the coordinates (in time and amplitude) of the above referred points. To assess the accuracy of the algorithm, a reference database of 173 pulses from eight volunteers, was established and the values yielded by the PPIA were compared to annotations from a human expert engineer (HEE). The quality of the results is statistically quantified either in time as in amplitude. Average values of 4.20% for error, 99.09% for sensitivity and 96.77% for positive predictive value were found to be associated to time information while amplitude yields averages of 2.68%, 99.08% and 98.22%, respectively, for the same parameters.

1 INTRODUCTION

Over the last years, increasing attention has been paid to the effect of arterial stiffness, the measure of rigidity of arteries (Mackenzie *et al*, 2002), on the development of cardiovascular (CV) diseases (Laurent *et al*, 2006).

The study of non-invasive methods that address this problem, using devices capable of precisely assessing the arterial pressure waveform (APW) remains a capital issue that mobilizes the interest of researchers. Pulse diagnosis has proved to be a convenient, inexpensive and painless diagnosis method; however experience has also shown that, in order to obtain reliable results, it may require practitioners with considerable training and experience (Avolio *et al*, 2010).

Historically, the cuff sphygmomanometer, universally used by clinicians since the beginning of

the 20th century, was the first device to quantify a part of the information contained in the APW and conquered a (still) irreplaceable role in general clinical practice. The measurement of pulse pressure, however, is the simplest surrogate measure of arterial stiffness.

Nevertheless, the APW contains a vast amount of pathophysiological information about the cardiovascular condition that is concealed in its morphology. Many factors can determine the contour of the APW: the blood volume ejected from the heart, the distensibility of the arterial vessel, runoff of the blood to the periphery, rate of the velocity of blood in the vessels and the vascular properties of the vessels (Oppenheim *et al*, 1995).

Although different technologies have been put to the service of this major endeavour, a short review of recent literature leads us to the conclusion that applanation tonometry (e.g. Sphygmocor® from

AtCor, West Ryde, Australia and PulsePen® from DiaTecne, Milan, Italy) remains the golden standard, only second to the invasive catheterization.

As for the technologies based on electromechanic sensors, PZ probes have been studied either for assessing timing parameters of the APW (McLaughlin *et al* 2003) or for monitoring APW at the radial artery (Clemente *et al* 2010). They also are in the basis of some commercial instruments dedicated to PWV assessment (e.g. Complior® from Artech-Medical, Pantin, France).

A number of beat detectors have been reported (Donelli *et al*, 2002 and Oppenheim *et al*, 1995) for characterizing APW in the literature; however the full delineation of APW remains a capital issue that motivates our investigation.

In a previous study carried out by our group, a piezoelectric probe for non-invasive arterial pressure waveform reproduction was developed.

In this paper an automatic delineator of the characteristic features of the APW, meant to works in articulation with the probe, is proposed. Its action relies on the coordinates (time vs. amplitude) of the 4 prominent points that can be identified in the APW: systolic peak (SP), reflection point (RP), dirotic peak (DP) and dirotic notch (DN).

2 PIEZOELECTRIC PROBE

In a previous study, a piezoelectric probe capable of recovering the arterial pressure was developed.

This device delivers as output, a high fidelity replica of the APW, free from baseline drift due to the action of a BLR circuit that avoids the need of offline removal algorithms for this purpose (Xu *et al*, 2007).

The elimination of baseline drift by the BLR circuit consists in forcing the foot of systolic pulses to start close to zero, without affecting the shape of the signal.

This action is triggered only at the end of the cardiac pulse, just before the starting of a new pulse.

Figure1 illustrates the main components of our pulse acquisition system: The PZ probe, left photograph, is held by a collar and placed in the carotid artery site for the *in vivo* data acquisition.

Signal conditioning and data acquisition (USB 6009 from National Instruments are enclosed in the electronics box (mid panel).

A personal computer running a dedicated software package with PPIA, shown in the right panel, completes the system.

3 METHODOLOGY

Once the foundations of our delineator are defined we assess the capability of the algorithm in identifying various prominent points from which the clinically relevant waveform features are computed.

To attain this goal, a small universe of eight healthy volunteers was organized as the seed of a larger data base of cardiac pulses to be build in the follow-up of this work.

The study protocol was approved by the ethical committee of *Centro Cirúrgico de Coimbra*, Portugal. All subjects were volunteers that previously granted a written informed consent.

A set of pulses was acquired from each volunteer followed by a pulse by pulse segmentation, routine, as depicted in figure 2. The onset of the waveform is identified in the signal conditioning circuit according the heart rate value.

3.1 Physiologic Foundation

Four prominent points are generally identifiable in a typical APW profile: SP, RP, DN and DP. Their physiological origin is briefly recalled in the following paragraphs.

The arterial pressure wave propagates along the arterial tree and, as its branches change in diameter



Figure 1: The main components of our non-invasive system for hemodynamic analysis. (a) PZ probe; (b) Acquisition box; (c) Graphical User Interface.

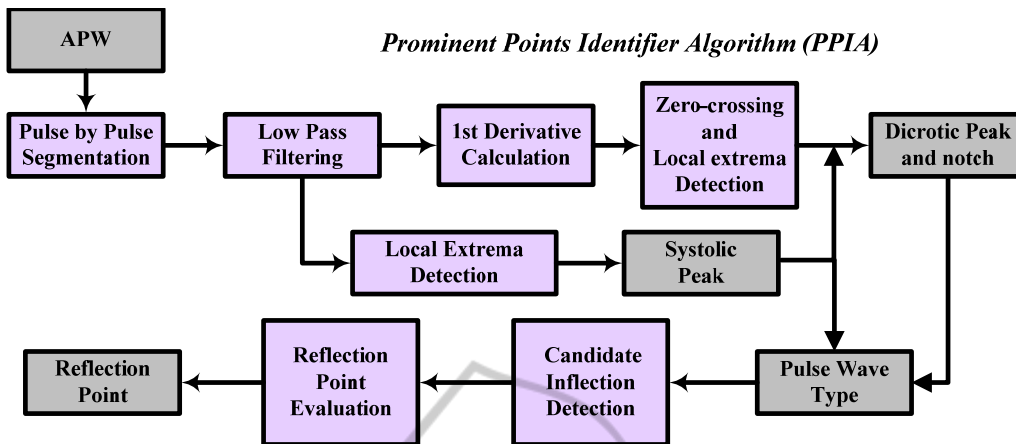


Figure 3: Flowchart of the PPIA.

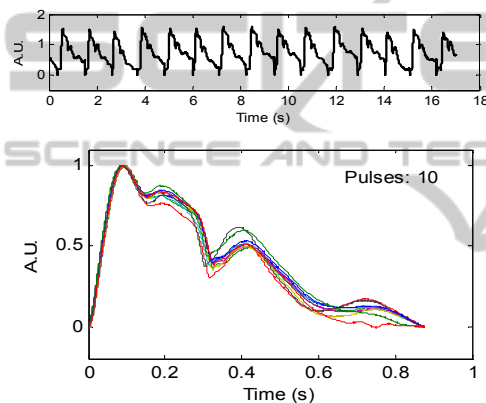


Figure 2: Set of carotid pulses and the corresponding pulse segments.

and stiffness, reflections of a portion of the original energy is sent back towards the heart.

The waves reflected from the periphery, superimpose to the forward wave originating a visible change in the APW profile which determines the RP.

Further to RP, the identification of the SP, simply defined as the point of maximum systolic pressure, allows the determination of a very important hemodynamic parameter that denotes the increase of pressure imparted by the reflected wave - the Augmentation Index (AI), (Almeida *et al*, 2010).

The aortic DN pulse is associated to the effect of the aortic valve closure when a small portion of ejected blood moves back to the left ventricle (Donelli *et al* 2002). This feature must be identified by the delineator in order to accurately determine the end of ventricular ejection, which is necessary for cardiac output determinations.

The pulse profile is characterized by two peaks, SP and the DP, one valley, DN, and one inflection,

RP. The PPIA must deal with the specification of each one of these shapes in order to produce an accurate identification of all four prominent points.

3.2 The Algorithm

As mentioned before, the main purpose of the algorithm is the identification (in time and relative amplitude) of the prominent points of the cardiac cycle and make them available for analysis in an understandable, clear way.

Flowchart of figure 3 depicts the main sequence of operations performed by our Prominent Points Identifier Algorithm (PPIA). The delineator is based on the combined analysis of APW and its first order derivative.

After acquiring a few pulses, around 10 in the example of figure 2, the pulses are subject to a segmentation process and normalised to the diastolic-systolic pressure interval.

The use of the first derivative curve justifies that, immediately following acquisition, a low pass filter is used to suppress high frequency noise that would, otherwise, turn the first derivative unusable. The 50Hz turn point of the filter ensures the interesting range of frequencies to ensure the visibility of the points. Figure 4 shows one pulse with its prominent points identified by the PPIA. As an example, the AI of the corresponding volunteer is also derived.

3.2.1 Systolic Peak (SP)

The SP identification is carried out using a local extreme identification routine (Billauer, 2008).

This routine detects a maximum only if the value of the previous minimum differs by a selectable minimum amount, referred to as delta.

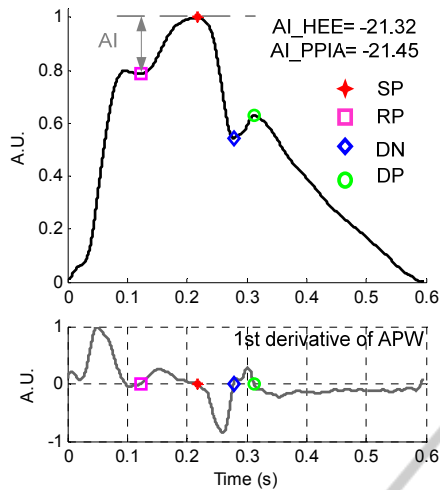


Figure 4: Example of type A pulse waveform and its prominent points identified by PPIA.

Since the cardiac cycle shows a variable number of local maxima (2 to 4 depending on wave type and artefacts), the routine must run repeatedly, with different values of delta, to ensure the correct identification of the SP.

3.2.2 Dicrotic Notch (DN) and Dicrotic Peak (DP)

The identification of the SP combined with the zero crossing values of the first order derivative is used to identify the dicrotic points (notch and peak) that must be located between the SP and the end of the pulse.

The oscillations that inevitably occur can mask the true DN and DP values. To prevent this, zero crossing information must be combined with the amplitude values of the APW pulse.

3.2.3 Waveform Type

According to the criteria proposed by Murgó *et al* (1980) the pressure waveform can be classified into one of four types (A, B, C, D) depending on the location of the reflected wave, as shown in table 1.

To achieve this, the algorithm analyses the waveforms deriving the number of maximum peaks of the 1st order derivative of the APW taking as reference the localization of the SP.

3.2.4 Reflection Point (RP)

The RP identification is carried out in three steps: the localization of candidates, the elimination of oscillations and the comparison with the APW amplitude.

Table 1: Classification proposed by Murgó *et al* (1980).

Type A	The RP occurs before SP
Type B	The RP occurs shortly before of the SP (a threshold must be defined)
Type C	The RP occurs after SP
Type D	The inflection point cannot be observed

3.2.5 Augmentation Index (AI)

Augmentation index (AI) is one of the most widely used indices to quantify the arterial stiffness, based on the measurement of the strength of the reflected wave relative to the total pressure waveform.

$$AI = \pm \frac{P_S - P_i}{P_S - P_D} \quad (1)$$

Where P_S is the APW peak pressure, P_i its pressure at the inflection point and P_D is the diastolic blood pressure.

Types A and B show positive values of AI denoting high arterial stiffness situations, while in type C waveforms the negative values of AI is characteristic of a relatively elastic and healthier artery condition.

The key point in estimating AI is the correct identification of the RP, to allow the subsequent assessment of the relative augmentation that the reflected wave imparts to the pressure waveform. Several methods have been described in the literature to evaluate this parameter. The algorithm developed in this work is compared with the classification of a human expert engineer (HEE) to understand the effect of wrong RP identifications in AI calculation.

3.3 Evaluation Procedure

To acquire the pulses we used a previously developed pulse probe and organised a small universe of eight volunteers from which a reference database was built up.

In a first step, we used the algorithm described above to identify the prominent points - SP, DN, DP and RP. A human expert engineer (HEE) carefully inspected each APW pulse and manually annotates the same points.

All points are classified in the three classic types: true positive (TP) and, just for the discrepant ones, false negative (FN) and false positive (FP). FNs occur only when the point cannot be identified.

The classification takes the HEE results as reference and uses the same 8 ms threshold adopted by others (Li *et al*, 2010 and Zong *et al*, 2003).

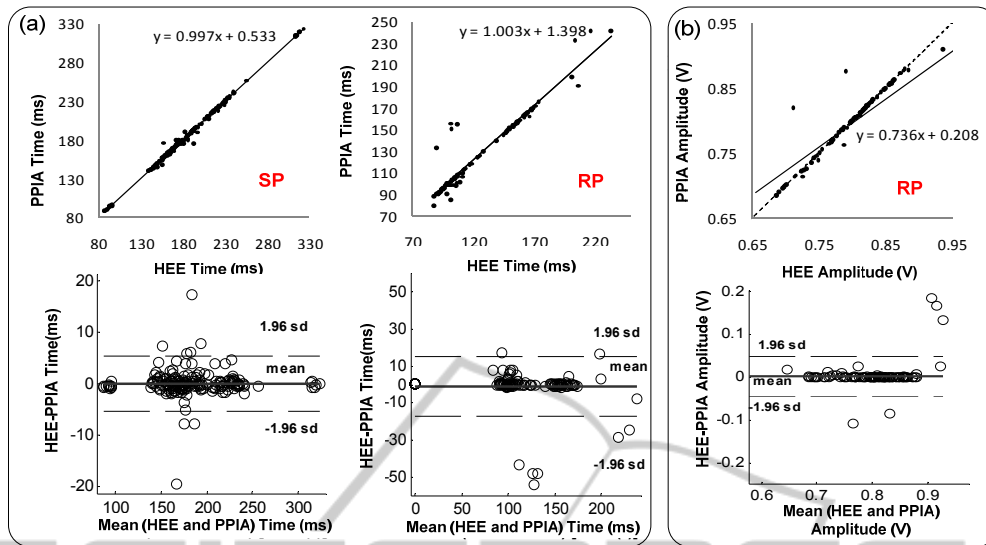


Figure 5: Agreement between the SP and RP obtained via PPIA and HEE (a) time information of SP and RP; (b) relative amplitude of RP. Regression plots (top) and Bland-Altman plots (bottom).

Sensitivity (S), positive predictive value (P^+) and error of the PPIA algorithm shown in table 1 are now computed according to:

$$S = \frac{TP}{TP+FN} \quad (2)$$

$$P^+ = \frac{TP}{TP+FP} \quad (3)$$

$$error = \frac{FP+FN}{TP+FP} \quad (4)$$

An identical procedure is carried out in the amplitude sense, using a 1% of pulse maximum, threshold.

4 RESULTS

Tables 2 and 3 show the sensitivity, positive predictive value and error of the algorithm for the time and amplitude information, respectively.

Statistical analysis was performed using Microsoft Excel® 2007 and SPSS® version 18.

As expected, RP shows the worst performance indices due to its inherent detection difficulty, either for the HEE as for the PPIA.

The three last columns of table 2 yield average values of 4.20%, 99.09% and 96.77 % for error, S and P^+ , respectively.

The same study applied to the amplitude information of table 3 yields averages of 2.68%, 99.08% and 98.22 %.

Table 2: Validation of PPIA performance (time information) compared to HEE annotations.

	Pulses	TP	FP	FN	Error (%)	S (%)	P^+ (%)
SP	173	171	2	0	1.15	100	98.84
DN	173	165	8	0	4.62	100	95.37
DP	173	169	4	0	2.31	100	97.69
RP	173	159	8	6	8.38	96.36	95.20

Table 3: Validation of PPIA performance (amplitude information) compared to HEE annotations.

	Pulses	TP	FP	FN	Error (%)	S (%)	P^+ (%)
SP	173	173	0	0	0	100	100.00
DN	173	171	2	0	1.15	100	98.84
DP	173	172	1	0	0.58	100	99.42
RP	173	158	9	6	8.98	96.34	94.61

Figure 5 a) shows the correlation between the reference HEE and PPIA values (SP and RP analysis), as well the corresponding Bland - Altman plots.

The straight line fittings for SP and RP show an excellent correlation, where R^2 is the square of the sample correlation coefficient, between both estimates ($R^2=0.996$ and $R^2=0.907$, respectively).

The PPIA, in average, overestimates the SP by 0.009 ms and underestimates the RP by 0.99 ms. To explain the 100 fold factor between the estimation errors for SP and RP one should bear in mind that, in the APW curve, SP is a peak while RP is an inflection. This circumstance makes the SP estimation much easier for the HEE as well as for the PPIA. Should the data base be large enough and

the SP error would tend to zero while RP would eventually converge to a minimum, non-zero, biased level. This, however, remains a hypothesis to be demonstrated in the follow-up of this work.

Another interesting consequence of the nature of SP and RP is that amplitude errors summarized in table 3 are much lower than the corresponding time errors (table 2). In fact as they are both associated to a peak and an inflection, the first derivative of the APW curve shows close-to-zero values in their vicinity, hence the small resulting estimation error. This fact is visible in figure 5 b) that shows the correlation between the reference HEE and PPIA values for RP analysis, as well the corresponding Bland - Altman plot.

In fact, as can be seen in figure 6, AI error, measured by the difference between AI values from HEE and PPIA, amounts to an average value of just 0.53 %.

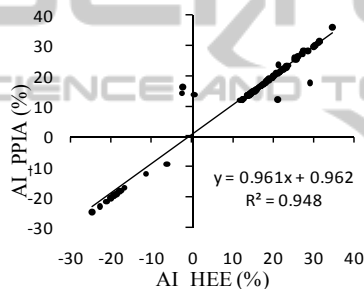


Figure 6: The relationships between AI obtained from PPIA and HEE.

Table 4: Statistics information of measurements depicted in figure 6.

Descriptive Statistics					
	Minimum	Maximum	Mean	Std.	
N	(%)	(%)	(%)	Deviation (%)	
Error	167	0.00	19.09	0.53	2.47

5 CONCLUSIONS

We described new automatic feature extraction algorithm capable of detecting the prominent points of the APW: SP, DN, DP and RP. This algorithm is a fundamental part of the automatic analysis tool in our non-invasive system for hemodynamic analysis.

The clinical use of our probe, however, will still require a medical oriented, multicenter study including comparison with standard methods, e.g. applanation tonometry and catheter collected data. The need for a larger data base has also emerged as the only means of attaining the necessary levels of confidence.

ACKNOWLEDGEMENTS

We acknowledge support from *Fundação para a Ciência e a Tecnologia* for funding (PTDC/SAU-BEB/100650/2008) and SFRH/BD/61356/2009) and from ISA, Intelligent Sensing Anywhere.

REFERENCES

- Almeida V., Pereira T., Borges E., Figueiras E., Cardoso J., Correia C., Pereira H. C., Malaquias J. L. and Simões J. B., 2009. Synthesized cardiac waveform in the evaluation of augmentation index algorithms. In IEEE EMB, *Proceedings of the 3rd International Joint Conference on Biomedical Engineering Systems and Technologies (BIOSTEC 2010)*. Valencia, Spain 20-23 January 2010.
- Avolio A. P., Butlin M., and Walsh A., 2010. Arterial blood pressure measurement and pulse wave analysis - their role in enhancing cardiovascular assessment. *Physiol. Meas.* 31, R1-R47.
- Billauer E., 2008. Peak detection using MATLAB. <http://www.billauer.co.il/peakdet.html>. [Accessed 13 July 2010]
- Clemente F, Arpaia P and Cimmino P 2010 A piezo-film-based measurement system for global haemodynamic assessment *Physiol. Meas.* 31 697-714.
- Laurent S., Cockcroft J., Van Bortel L., Boutouyrie P., Giannattasio C., Hayoz D., Pannier B., Vlachopoulos C., Wilkinson I., and Struijker-Boudier H., 2006. Expert consensus document on arterial stiffness: methodological issues and clinical applications. *European Heart Journal*, 27, 2588-2605.
- Li, B. N., Dong, M. C., Vai, M. I., 2010. On an automatic delineator for arterial blood pressure waveforms. *Biomedical Signal Processing and Control*, 5, 76-81.
- Oppenheim, M. J., Sittig, D. F., 1995. An innovative dirotic notch detection algorithm which combines rule-based logic with digital signal processing techniques. *Computers and biomedical research*, 28, 154-170.
- Mackenzie I. S., Wilkinson I. B. and Cockcroft J. R., 2002. Assessment of arterial stiffness in clinical practice. *Q J Med.*, 95, 67-74.
- Robinson L., 1961 Reduction of Baseline Shift in Pulse-Amplitude Measurements. *Rev. Sci. Instr.* 32, 1057.
- Xu, L., Zhang, D., Wang, K., Li, N., Wang, X., 2007. Baseline wander correction in pulse waveforms using wavelet-based cascaded adaptive filter. *Computers in Biology and medicine*, 37, 716-731.
- Zong, W., Heldt, T., Moody, G.B., Mark, R.G., 2003. An open source algorithm to detect onset of arterial blood pressure pulses. *Computers in Cardiology*, 30, 259-262.